the shear band should be responsible for the initiation of microcracks.

3 Conclusions

1) Highly localized shear bands can be observed at the angle of about 45° with respect to loading axis in the as-extruded WHAs.

2) The sensitivity to adiabatic shear banding exhibits a notably increasing tendency with the increase in extrusion ratio due to the rising flow stress.

3) The microcracks occur along the shear stress direction near the centre of the shear band and initiate at the interface of W-M as well as the interior of tungsten.

4) The dislocation pile-ups exist at the interface of W-M, and microcracks propagate along the boundary and inside of the subgrain in the interior of tungsten within the shear band.

References

1 Bai Y, Dodd B. *Adiabatic Shear Localization-Occurrence, Theories and Application*[M]. Oxford: Pergamon Press, 1992

2 Wright T W. *The Physics and Mathematics of Adiabatic Shear Bands*[M]. Cambridge: Cambridge University Press, 2002

3 Meyers M A. *Dynamic Behavior of Materials*[M]. New York: John Wiley & Sons, 1994

4 Xu Y B, Zhang J H, Bai Y L *et al. Metall Trans A*[J], 2008, 39A: 811

5 Magness L S, Kapoor D, Dowding R. *Mater Manuf Processes*[J], 1995, 10: 531

6 Cai W D, Li Y, Dowding R *et al. Rev Particulate Mater*[J], 1995, 3: 71

7 Kim D K, Lee S, Noh J W. *Mater Sci Eng A*[J], 1998, 247: 285

8 Wu G C, You Q, Wang D. *Int. J Refract Mater*[J], 1999, 17: 299

9 Ekbom L, Antonsson T. *Int J Refract Mater*[J], 2002, 20: 375

10 Sanghyun P, Kim D K, Lee S. *Mater Sci Eng A*[J], 2003, 363: 179

11 Randall M G, Olevsky E. *Int J Refract Mater*[J], 2005, 23: 77

12 Liu Jinxu, Li Shukui, Zhou Xiaoqing *et al. Scripta Mater*[J], 2008, 59: 1271

13 Rogers H C. *Ann Rev Mater Sci*[J], 1979, 9: 283

14 Me-Bar Y, Shechtman D. *Mater Sci Eng*[J], 1983, 58: 181

15 Affouard J L, Dormeval R, Stelly M *et al.* In: Harding J ed. *3rd Conf Mechanical Properties of Materials at High Rates of Strain*, Bristol: Institute of Physics, 1984: 533

16 Xu Y B, Wang Z G, Huang X L *et al. Mater Sci Eng A*[J], 1989, 114: 81

17 Xu Y B, Bai Y L, Xue Q *et al. Acta Mater*[J], 1996, 44: 1917

18 Zhou M, Rosakis A J, Ravichandran G. *J Mech Phys Solids*[J], 1996, 44: 981

19 Guduru P R, Rosakis A J, Ravichandran G. *Mechanics of Materials*[J], 2001, 33: 371

20 Xu Y B, Zhong W L, Chen Y J *et al. Mater Sci Eng A*[J], 2001, 299: 287

21 Zhang Zhaohui, Wang Fuchi, Li Shukui *et al. Mater Sci Eng A*[J], 2006, 435: 632

22 Liu Jinxu, Li Shukui, Fan Ailing *et al. Mater Sci Eng A*[J], 2008, 487: 235

挤压态钨合金绝热剪切局域化及微裂纹萌生现象研究

彭　磊，李树奎，周晓青，才鸿年

(北京理工大学，北京 100081)

摘　要：研究变形量对挤压态钨合金动态力学行为的影响及钨合金绝热剪切带内的微观开裂行为。结果表明，加载方向垂直于纤维取向时，随变形量由0增加至40.8%，挤压态钨合金绝热剪切敏感性显著增大；由对钨合金绝热剪切带内微观组织的SEM观察可知，靠近绝热剪切带中心处出现在微裂纹且微裂纹萌生于W-M界面及W颗粒内部；进一步的TEM观察可知，剪切带内W-M界面处存在大量的位错塞积，W颗粒中则出现亚晶内部及沿亚晶界扩展的微裂纹。

关键词：钨合金；挤压；绝热剪切带；微裂纹萌生

作者简介：彭　磊，男，1983年生，博士生，北京理工大学材料科学与工程学院，北京 100081，电话：010-68913951，E-mail: penglei@bit.edu.cn

Rare Metal Materials and Engineering
Volume 39, Issue 12, December 2010
Online English edition of the Chinese language journal

Available online at www.sciencedirect.com
ScienceDirect

Cite this article as: Rare Metal Materials and Engineering, 2010, 39(12): 2084-2087.

ARTICLE

Adiabatic Shear Localization and Microcracks Initiation in an Extruded Tungsten Heavy Alloy

Peng Lei, Li Shukui, Zhou Xiaoqing, Cai Hongnian

Beijing Institute of Technology, Beijing 100081, China

Abstract: The influence of extrusion deformation ratio on the dynamic mechanical behavior in a tungsten heavy alloy was investigated under uniaxial compression with loading direction perpendicular to the fiber orientation. With extrusion deformation ratio increasing from 0 to 40.8%, the sensitivity of adiabatic shear banding shows an obviously rising tendency. Microcracks could be seen near the centre of the shear band and initiate at the interface of tungsten-matrix as well as the interior of tungsten. Moreover, the observation by the transmission electron microscopy reveals the dislocation pile-ups at the interface of tungsten-matrix and the presence of a microcrack propagating along the boundary and inside of the subgrain in the interior of tungsten within the shear band.

Key words: tungsten heavy alloy; extrusion; adiabatic shear bands; microcrack initiation

Adiabatic shear localization is often observed after large plastic deformations in metals, polymers and powders. The shear bands, as a form of large plastic deformation, are usually the precursors to fracture[1-4]. The adiabatic shear localization is of critical importance in many applications including explosive fragmentation, high-speed machining, and kinetic energy penetrators. In particular, the kinetic energy penetrators made of tungsten heavy alloys (WHAs) require that the materials have good susceptibility of adiabatic shear banding to exhibit "self-sharpening" behavior under high strain rates[5, 6]. As a result, a great deal of work has been done to investigate variables affecting the sensitivity of WHAs to shear localization[7-11]. We also have reported that the susceptibility of WHAs processed by hydrostatic extrusion and torsion could be influenced by the torsion deformation ratio, and the susceptibility shows a rising tendency with the increase in torsion deformation ratio[12].

Furthermore, it is generally assumed that the fracture induced by the adiabatic shear localization might be the consequence of the accumulation of microscopic damage involved in adiabatic shear banding because of the large plastic deformations within a band[1]. The microscopic damage related to adiabatic shear band has been observed in U-2Mo[13], Ti-6Al-4V[14], steels[15-19], 8090 Al-Li alloy[20], etc.

However, no experimental information is currently available on extrusion ratio sensitivity of the adiabatic shear banding in WHAs. Such information would be of considerable use for the ductility of WHAs processed by extrusion and torsion which could be determined by extrusion ratio at a given torsion deformation ratio. And ductility is a key parameter for the penetrator alloy. Moreover, the microscopic damage involved in the adiabatic shear banding of WHAs still remains unknown. This paper describes the investigation on the effect of extrusion ratio on the sensitivity of the adiabatic shear localization in a tungsten heavy alloy, and the observations of the microscopic damage within the shear band are also reported.

1 Experimental procedure

In the present study, the initial material investigated was liquid-phase sintered 93W-4.9Ni-2.1Fe (mass fraction, %). The as-sintered WHA rods were then deformed by hydrostatic extrusion with different deformation ratios at room temperature. The specimens with various extrusion ratios were named as specimen 1, 2, 3 and 4, respectively, as shown in Table 1. Further details on preparation of the alloys can be found in Zhang *et al*[21].

The uniaxial dynamic compression experiments were carried out on the WHAs using a Split Hopkinson Pressure Bar

Received date: December 20, 2009
Corresponding author: Peng Lei, Candidate for Ph. D., School of Material Science and Engineering, Beijing Institute of Technology, Beijing 100081, P. R. China, Tel: 0086-10-68913951, E-mail: penglei@bit.edu.cn

Table 1 Experimental parameters of hydrostatic extrusion deformation

Specimen	Diameter of WHA rod/mm		Deformation ratio/%
	Before extrusion	After extrusion	
1	10	10	0
2	11	10	17.4
3	12	10	30.6
4	13	10	40.8

(SHPB). The loading direction perpendicular to the fiber orientation was selected for the high sensitivity to adiabatic shear banding[22], which could be assumed to investigate the influence of extrusion ratio on the sensitivity to adiabatic shear banding in axial specimens (loading direction parallel to the fiber orientation) at the same torsional angle of 90°. Cylindrical specimens (5 mm in diameter ×5 mm) were cut off from the hydrostatic extrusion WHA rods by wire electrical discharge machining with the 90° angle between the cylinder axis and the extrusion direction. Two different speeds of incident bar were used to produce two different strain rates of about 3500 s^{-1} and 4000 s^{-1} in specimens. The specimens tested under SHPB were processed by standard sample preparation techniques for the electron metallographic observations. Scanning electron microscopy (SEM) and transmission electron microscopy (TEM) were then employed to reveal the plastic flow in the WHAs.

2 Results and Discussion

2.1 Influence of extrusion deformation ratio on the sensitivity to adiabatic shear localization

Fig. 1 displays the typical true stress-strain behavior of various specimens obtained from repeated uniaxial dynamic compression tests. Obviously, the flow stress increases with increasing of extrusion ratio due to the stronger strain hardening. The stress-strain curves of as-extruded specimens show almost the same trend, and the softening exhibits an apparent rising tendency with increasing of extrusion ratio, while the as-sintered specimen indicates evident strain hardening. Furthermore, it should be pointed out that the stress unloading of specimens 1 and 2 are due to the ending of pulse duration without fracture, while the cracks at an angle of about 45° with respect to loading direction result in the stress unloading of specimens 3 and 4. The obvious flow softening and fracture mode of the as-extruded specimens strongly suggest that the shear localization probably occur during the uniaxial dynamic compression tests.

In order to examine the plastic flow in the WHAs, specimens 1, 2, 3 and 4 were sectioned along the compression axis, ground, polished and etched. Fig.2a-2d shows the SEM images of the specimens after loading at the strain rate of about 4000 s^{-1}. Uniform plastic deformation can be clearly seen in the as-sintered specimen, as shown in Fig.2a; while the

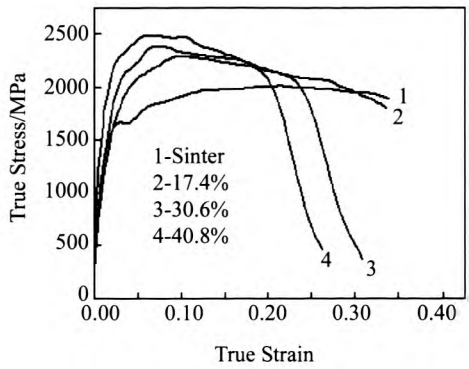

Fig.1 True stress-strain curves of the WHAs with various extrusion ratios under uniaxial dynamic compression. The strain rate is about 4000 s^{-1} and loading direction is perpendicular to the fiber orientation

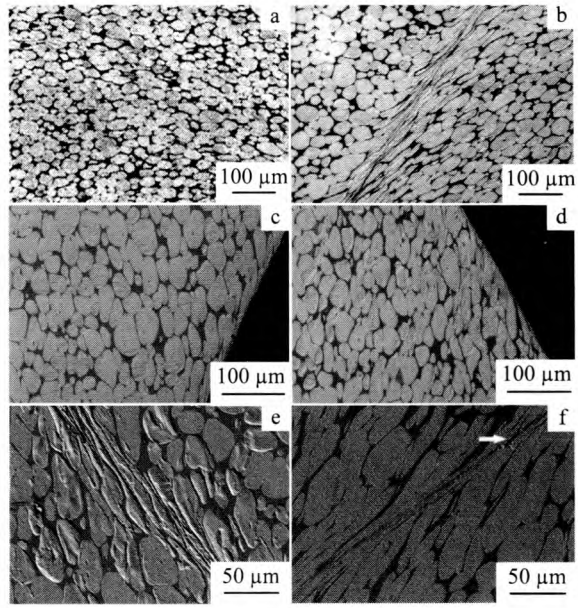

Fig.2 SEM images of uniform plastic deformation in the as-sintered WHA and shear localization in the as-extruded WHAs under uniaxial dynamic compression. The arrow in (f) indicates the presence of the microcrack in the shear band: (a-d) specimen 1-4, under the strain rate of about 4000s^{-1}; (e-f) specimen 3-4, under the strain rate of about 3500 s^{-1}

as-extruded specimens exhibit obvious shear localization: an adiabatic shear band (ASB) at an angle of approximately 45° relative to loading direction in specimen 2 (Fig. 2b) and the fracture induced by shear localization adjacent to the fracture surface in specimen 3 and 4 (Fig. 2c and 2d). The plastic flow in specimen 3 and 4 which is not fractured at the lower strain rate of about 3500 s^{-1} can be also observed. Fig. 2e and 2f reveal the shear localization found in specimen 3 and 4 under this condition and it is clearly observed that the width of the ASB in specimen 4 (about 15-20 μm) is narrower than that in

specimen 3 (about 25-30 μm), implying the better sensitivity to the adiabatic shear banding of specimen 4. The crack followed by shear localization could even be seen near the centre of ASB in specimen 4, as indicated by the arrow in Fig. 2f. Combining Fig. 1 with Fig. 2, we can conclude that the susceptibility of hydrostatic extrusion WHAs to the adiabatic shear banding increases with increasing of extrusion ratio when loading direction is perpendicular to fiber orientation.

The adiabatic temperature rise (ΔT) during the dynamic loading can be calculated as:

$$\Delta T = \frac{\beta}{\rho C_p} \int_0^{\varepsilon_f} \sigma \, d\varepsilon \quad (1)$$

where β is the Taylor-Quinney coefficient which characterizes the portion of plastic work converted into heat, and ρ, C_P, σ, ε_f represent density, specific heat, flow stress, true strain, respectively. For specimens 1-4, β, ρ and C_P are all the same. Therefore, according to Eq.(1), the adiabatic temperature rise in the specimens increases with increasing of extrusion ratio at a given ε_f due to rising of σ.

Because such a temperature rise could lead to considerable flow softening in dynamic compression, the sensitivity of adiabatic shear banding increases with rising of extrusion ratio.

2.2 Microcracks initiation in shear band

Fig. 3 illustrates the details of microscopic damage within the shear band which is seen in Fig. 2f. As shown in Fig. 3a, microcracks are parallel to the shear band and the width of the shear band is uneven: near the crack tip, the width is about 15 μm; apart from the crack zone, it has a width of about 20 μm. On the other hand, the damage appears to be stronger when nearer the center of the band. In one word, the crack zone undergoes more severe plastic deformation. Thus, it can be assumed that the large strain and stress concentration in the shear band should be responsible for the formation of microcracks. The close-up views of the microcracks are displayed in Fig. 3b and 3c. From these micrographs, it could be found that the microcracks initiate at the interface of tungsten (W)-matrix (M) (indicated by the white arrows in Fig. 3b) as well as the interior of tungsten (indicated by the black arrows in Fig. 3c). In addition, the rotation and the distortion of the microcracks resulting from severe shear could also be seen. The accumulation of a large quantity of microcracks may result in the eventual fracture.

Fig. 4 exhibits the TEM image of the interface between tungsten and matrix in the shear band. The apparent dislocation pile-ups could be seen at the interface. It can be assumed that when deformation continues, the high flow stress induced by dislocation pile-ups will exceed the W-M bonding strength and finally make the microcrack initiation at the interface, as mentioned in Fig. 3b. The interior of the tungsten within the shear band can be observed in Fig. 5. The grains are elongated to strips with the width of about 200 nm and tend to be aligned

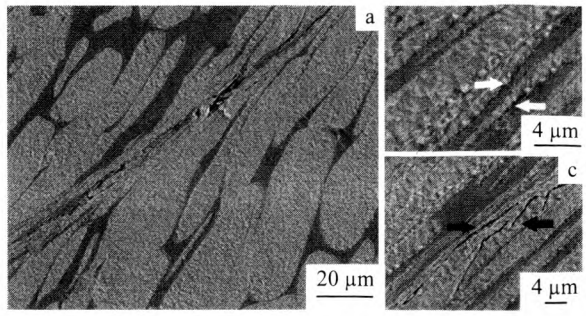

Fig.3 SEM images of microcracks initiation within the shear band: (a) low magnification, (b) and (c) high magnification. The microcracks initiate at the interface of W-M shown as the white arrows in (b) and the interior of tungsten shown as the black arrows in (c)

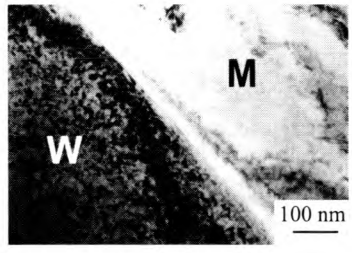

Fig.4 TEM image of dislocation pile-ups at the interface of W-M in the shear band

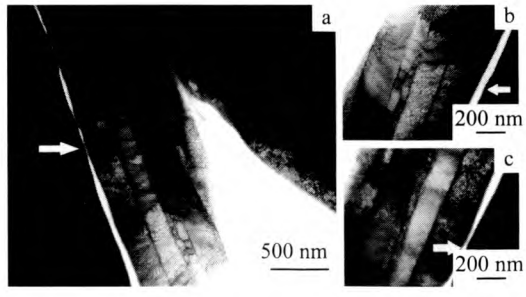

Fig.5 TEM images of elongated subgrains and a microcrack (shown as the white arrows) in the interior of tungsten within the shear band: (a) subgrains and microcrack, (b) microcrack propagating along the boundary and (c) the inside of the subgrain

along the shear stress direction. The other visible issue is the presence of a microcrack which propagates along the boundary (Fig. 5b) and the inside (Fig. 5c) of the subgrain. Due to the high density of dislocations at the subgrain boundary, we may infer that the microcrack first nucleates at the subgrain boundary and then propagates into the interior of the subgrain. Altogether, it might be anticipated that the large strain and the stress concentration resulting from the dislocation pile-ups at the interface of W-M and the subgrain boundary in W within